

PARTICLE-BASED ALGORITHM FOR STOCHASTIC OPTIMAL CONTROL

SEBASTIAN REICH

ABSTRACT. The solution to a stochastic optimal control problem can be determined by computing the value function from a discretization of the associated Hamilton–Jacobi–Bellman equation. Alternatively, the problem can be reformulated in terms of a pair of forward-backward SDEs, which makes Monte–Carlo techniques applicable. More recently, the problem has also been viewed from the perspective of forward and reverse time SDEs and their associated Fokker–Planck equations. This approach is closely related to techniques used in diffusion-based generative models. Forward and reverse time formulations express the value function as the ratio of two probability density functions; one stemming from a forward McKean–Vlasov SDE and another one from a reverse McKean–Vlasov SDE. In this paper, we extend this approach to a more general class of stochastic optimal control problems and combine it with ensemble Kalman filter type and diffusion map approximation techniques in order to obtain efficient and robust particle-based algorithms.

1. INTRODUCTION

We consider controlled nonlinear diffusion processes of the form

$$(1) \quad dX_t = b(X_t)dt + G(X_t)u_tdt + \sigma(X_t)dB_t, \quad X_0 = x_0.$$

Here $X_t \in \mathbb{R}^{d_x}$ denotes the random state variable at time $t \geq 0$ and $B_t \in \mathbb{R}^{d_b}$ standard d_b -dimensional Brownian motion. Furthermore, the functions $b(x) \in \mathbb{R}^{d_x}$, $G(x) \in \mathbb{R}^{d_x \times d_u}$, and $\sigma(x) \in \mathbb{R}^{d_x \times d_b}$ are all assumed to be given.

The cost to optimize via an appropriate choice of the time-dependent control $u_{0:T} = \{u_t\}_{t \in [0, T]}$ is given by

$$(2) \quad J_T(x_0, u_{0:T}) = \mathbb{E} \left[\int_0^T \left(c(X_t) + \frac{1}{2} u_t^T R^{-1} u_t \right) dt + f(X_T) \right].$$

Expectation is taken with regard to the path measure generated by the stochastic differential equation (SDE) (1) conditioned on the initial $X_0 = x_0$ and a given control law $u_{0:T}$, which we assume to be state-dependent. Here

$$(3) \quad c(x) = \frac{1}{2} h(x)^T S^{-1} h(x)$$

denotes the running cost and

$$(4) \quad f(x) = \frac{1}{2} \xi(x)^T V^{-1} \xi(x)$$

Date: February 29, 2024.

the terminal cost. The matrices $R \in \mathbb{R}^{d_u \times d_u}$, $S \in \mathbb{R}^{d_h \times d_h}$, $V \in \mathbb{R}^{d_\xi \times d_\xi}$ as well as the functions $h(x) \in \mathbb{R}^{d_h}$, $\xi(x) \in \mathbb{R}^{d_\xi}$ are again all assumed to be given. See [18] for an introduction to diffusion processes and [5, 17] for an introduction to stochastic control.

In this paper, we aim at finding control laws of the form

$$(5) \quad u_t(x) = RG(x)^T(A_t x + c_t),$$

which provide good approximations to the optimal feedback control law denoted here by $u_t^*(x)$. While the optimal control law can be found via the associated Hamilton–Jacobi–Bellman (HJB) equation [5]; solving such a PDE is computationally demanding [10]. Popular alternatives include those based on forward-backward SDEs [6] in combination with machine learning techniques [9, 10]. Here we follow the work of [15] instead, which in turn has been inspired by [2, 20, 16], to reformulate the problem in terms of two McKean–Vlasov SDEs over state space \mathbb{R}^{d_x} . Those SDEs need to be solved in forward and reverse time, respectively, only once and are related to generative models using diffusion processes [22, 23]. Furthermore, in order to obtain robust and easy to compute approximations, we employ the ensemble Kalman filter (EnKF) methodology to approximate the arising McKean–Vlasov interaction terms [11, 4]. A related EnKF-based approach to optimal control has been considered in [13] and is based on a direct approximation of the HJB equation via a McKean–Vlasov SDE. We use stabilization of an inverted pendulum position [17] to demonstrate the efficiency of our method. While the numerical experiments in [15] and [13] utilize ensemble sizes on the order of 10^3 , our method has been implemented with an ensemble of size $M = d_x + 1 = 3$. We also propose a more general methodology which combines the EnKF methodology with diffusion map approximations for the arising grad-log density terms [7, 8]. This extension is useful whenever the underlying densities cannot be approximated well by Gaussian distributions. We will illustrate this aspect through a controlled nonlinear Langevin dynamics process.

The remainder of this paper is structured as follows. The mathematical background on the HJB equation for stochastic optimal control problems is summarized in Section 2. We demonstrate in Section 3 how the value function defined by the HJB equation can be expressed as the ratio of two probability density functions. Here we extend previous work [15] to the wider class of optimal control problems defined by (1) and (2). Both the associated forward and reverse time evolution equations can be expressed in terms of McKean–Vlasov SDEs in the state variable, x . Before discussing numerical approximations of those McKean–Vlasov equations in Section 5, we demonstrate in Section 4 how our formulation is related to generative modeling using diffusion processes [22, 23]. We first discuss numerical approximations using EnKF-type methodologies [11, 4] in Section 5.1. Next we also employ diffusion maps [7, 8] in order to approximate grad-log density terms in Subsection 5.2. Numerical implementation details are discussed in Subsection 5.3, while numerical results for an inverted pendulum and nonlinear Langevin dynamics are presented in Section 6. Possible extension of the proposed methodology to infinite horizon optima control problems are discussed in Appendix 8.

2. MATHEMATICAL PROBLEM FORMULATION

In this section, we recap the essential aspects of finding the optima control law, $u_t^*(x)$, for controlled SDE (1) with cost (2). See [5, 17] for more detailed expositions.

The law, π_t , of the diffusion process, X_t , defined by the SDE (1) satisfies the Fokker–Planck equation

$$(6a) \quad \partial_t \pi_t = -\nabla_x \cdot (\pi_t (b + Gu_t)) + \frac{1}{2} \nabla_x \cdot (\pi_t \Sigma)$$

$$(6b) \quad = -\nabla_x \cdot \left(\pi_t \left(b + Gu_t - \frac{1}{2} \nabla_x \cdot \Sigma - \frac{1}{2} \Sigma \nabla_x \log \pi_t \right) \right),$$

where

$$(7) \quad \Sigma(x) = \sigma(x) \sigma(x)^\top.$$

We also introduce the weighted norm $\|\cdot\|_R$ via

$$(8) \quad \|u\|_R^2 = u^\top R^{-1} u.$$

Let the function $y_t(x)$ satisfy the backward HJB equation

$$(9) \quad -\partial_t y_t = (b + Gu_t) \cdot \nabla_x y_t + \frac{1}{2} \Sigma : D_x^2 y_t + c + \frac{1}{2} \|u_t\|_R^2$$

with terminal condition $y_T = f$. Here $D_x^2 y_t(x) \in \mathbb{R}^{d_x \times d_x}$ denotes the Hessian of $y_t(x)$ and $A : B = \text{tr}(AB^\top)$ the Frobenius inner product of two $d_x \times d_x$ matrices A and B . The optimal feedback control is provided by

$$(10) \quad u_t^*(x) = -RG(x)^\top \nabla_x y_t^*(x),$$

where the optimal value function $y_t^*(x)$ satisfies the HJB equation

$$(11a) \quad -\partial_t y_t^* = b \cdot \nabla_x y_t^* + \frac{1}{2} \Sigma : D_x^2 y_t^* + c + \min_u \left(Gu \cdot \nabla_x y_t^* + \frac{1}{2} \|u\|_R^2 \right)$$

$$(11b) \quad = b \cdot \nabla_x y_t^* + \frac{1}{2} \Sigma : D_x^2 y_t^* + c - \frac{1}{2} \|RG^\top \nabla_x y_t^*\|_R^2.$$

We apply the Cole–Hopf transformation and introduce the new function

$$(12) \quad v_t^*(x) := \exp(-y_t^*(x))$$

in order to obtain the transformed HJB equation

$$(13a) \quad -\partial_t v_t^* = b \cdot \nabla_x v_t^* + \frac{1}{2} \Sigma : D_x^2 v_t^*$$

$$(13b) \quad - \left(c + \frac{1}{2} \|\sigma^\top \nabla_x \log v_t^*\|^2 + \min_u \left(\frac{1}{2} \|u\|_R^2 - Gu \cdot \nabla_x \log v_t^* \right) \right) v_t^*$$

$$(13c) \quad = b \cdot \nabla_x v_t^* + \frac{1}{2} \Sigma : D_x^2 v_t^*$$

$$(13d) \quad - \left(c + \frac{1}{2} \|\sigma^\top \nabla_x \log v_t^*\|^2 - \frac{1}{2} \|RG^\top \nabla_x \log v_t^*\|_R^2 \right) v_t^*.$$

The terminal condition is $v_T^* = \exp(-f)$. Here we have used

$$(14) \quad \partial_t y_t^* = \frac{-1}{v_t^*} \partial_t v_t^*, \quad \nabla_x y_t^* = \frac{-1}{v_t^*} \nabla_x v_t^*, \quad \Sigma : D_x^2 y_t^* = \frac{-1}{v_t^*} \Sigma : D_x^2 v_t^* + \|\sigma^\top \nabla_x \log v_t^*\|^2.$$

The optimal control is now characterized by

$$(15) \quad u_t^*(x) = RG(x)^T \nabla_x \log v_t^*(x).$$

Remark 2.1. *The transformed HJB equation (13) simplifies to*

$$(16) \quad -\partial_t v_t^* = b \cdot \nabla_x v_t^* + \frac{1}{2} \Sigma : D_x^2 v_t^* - c v_t^*$$

for the special case $G = \sigma$ and $R = I$ and (13) becomes linear in v_t^* . This well-known fact has been exploited in the numerical work of [15]. Furthermore, the transformed HJB equation arising from the further simplification $c(x) \equiv 0$ leads to the standard backward Kolmogorov equation [18].

3. MCKEAN-VLASOV FORMULATION

In this section, we extend the McKean-Vlasov forward-reverse time approach to optimal control from [15] to more general control problems defined by (1) and (2). The first step is to choose an appropriate, potentially time-dependent convex cost function $\alpha_t(x)$ and to formulate a suitable evolution equation for the density

$$(17) \quad \tilde{\pi}_t := Z_t^{-1} v_t^* \bar{\pi}_t,$$

where v_t^* satisfies (13) and $\bar{\pi}_t$ the forward evolution equation

$$(18) \quad \partial_t \bar{\pi}_t = -\nabla_x \cdot (\bar{\pi}_t \bar{b}_t) - \bar{\pi}_t (\alpha_t - \bar{\pi}_t [\alpha_t])$$

with initial distribution $\bar{\pi}_0 = \delta_{x_0}$ and modified drift function

$$(19) \quad \bar{b}_t(x) := b(x) - \frac{1}{2} (\nabla_x \cdot \Sigma(x) + \Sigma(x) \nabla_x \log \bar{\pi}_t(x)).$$

The normalization constant Z_t is given by

$$(20) \quad Z_t = \bar{\pi}_t[v_t^*]$$

and δ_{x_0} denotes the Dirac delta function centered at x_0 . We note that

$$(21) \quad -\nabla_x \cdot (\bar{\pi}_t \bar{b}_t) = -\nabla_x \cdot (\bar{\pi}_t b) + \frac{1}{2} \nabla_x \cdot (\nabla_x \cdot (\bar{\pi}_t \Sigma)).$$

We next need to find an evolution equations for the probability density $\tilde{\pi}_t$ defined by (17). Relying on

$$(22) \quad \nabla_x \log \tilde{\pi}_t(x) = \nabla_x \log v_t^* + \nabla_x \log \bar{\pi}_t,$$

we introduce the modified drift

$$(23a) \quad \tilde{b}_t(x) := -\bar{b}_t(x) - \frac{1}{2} \Sigma(x) \nabla_x \log v_t^*(x)$$

$$(23b) \quad = -\bar{b}_t(x) - \frac{1}{2} \Sigma(x) (\nabla_x \log \tilde{\pi}_t(x) + \nabla_x \log \bar{\pi}_t(x))$$

$$(23c) \quad = -b(x) + \nabla_x \cdot \Sigma(x) + \Sigma(x) \nabla_x \log \bar{\pi}_t(x)$$

$$(23d) \quad - \frac{1}{2} (\nabla_x \cdot \Sigma(x) + \Sigma(x) \nabla_x \cdot \log \tilde{\pi}_t(x)).$$

We note that

$$(24) \quad -\nabla_x \cdot (\tilde{\pi}_t \tilde{b}_t) = \nabla_x \cdot (\tilde{\pi}_t (b - \nabla_x \cdot \Sigma - \Sigma \nabla_x \log \bar{\pi}_t)) + \frac{1}{2} \nabla_x \cdot (\nabla_x \cdot (\tilde{\pi}_t \Sigma)),$$

which leads naturally to the interpretation in terms of a reverse time SDE with McKean–Vlasov-type drift function. Before investigating this aspect in more detail, we state the following lemma, which links the modified drift \tilde{b}_t with the time evolution of the probability density $\tilde{\pi}_t$ defined by (17).

Lemma 3.1. *Given the forward evolution equation (18) and the HJB equation (13), the probability density defined by (17) satisfies the reverse time evolution equation*

$$(25) \quad -\partial_t \tilde{\pi}_t = -\nabla_x \cdot \left(\tilde{\pi}_t \tilde{b}_t \right) - \tilde{\pi}_t \left(c - \alpha_t + \frac{1}{2} \|\sigma^T \nabla_x \log v_t^*\|^2 - \frac{1}{2} \|RG^T \nabla_x \log v_t^*\|_R^2 - \zeta_t \right)$$

with terminal condition $\tilde{\pi}_T = Z_T^{-1} \exp(-f) \bar{\pi}_T$, where ζ_t is an appropriate normalization constant.

Proof. Since (23) and

$$(26) \quad \nabla_x \cdot (\Sigma \nabla_x v_t^*) = \nabla_x v_t^* \cdot (\nabla_x \cdot \Sigma) + \Sigma : D_x^2 v_t^*,$$

and assuming that (17) holds, it follows that

$$(27a) \quad -\nabla_x \cdot (\tilde{\pi}_t \tilde{b}_t) = \nabla_x \cdot \left(\tilde{\pi}_t \left(\bar{b}_t + \frac{1}{2} \Sigma \nabla_x \log v_t^* \right) \right)$$

$$(27b) \quad = \frac{v_t^*}{Z_t} \nabla_x \cdot (\bar{\pi}_t \bar{b}_t) + \frac{\bar{\pi}_t}{Z_t} (\Sigma \nabla_x v_t^*) \cdot \bar{b}_t + \frac{1}{2Z_t} \nabla_x \cdot (\bar{\pi}_t \Sigma \nabla_x v_t^*)$$

$$(27c) \quad = \frac{v_t^*}{Z_t} \nabla_x \cdot (\bar{\pi}_t \bar{b}_t) + \frac{\bar{\pi}_t}{Z_t} \left(\nabla_x v_t^* \cdot \left(\bar{b}_t - \frac{1}{2} \nabla_x \cdot \Sigma \right) + \frac{1}{2} \nabla_x \cdot (\Sigma \nabla_x v_t^*) \right)$$

$$(27d) \quad = \frac{v_t^*}{Z_t} \nabla_x \cdot (\bar{\pi}_t \bar{b}_t) + \frac{\bar{\pi}_t}{Z_t} \left(\bar{b}_t \cdot \nabla_x v_t^* + \frac{1}{2} \Sigma : D_x^2 v_t^* \right).$$

Hence it holds indeed that

$$(28) \quad \partial_t \tilde{\pi}_t = \frac{v_t^*}{Z_t} \partial_t \bar{\pi}_t + \frac{\bar{\pi}_t}{Z_t} \partial_t v_t^* - \frac{\tilde{\pi}_t}{Z_t} \frac{dZ_t}{dt}$$

for the partial time derivatives given by (25), (18), and (13), respectively. Furthermore, $\tilde{\pi}_T = v_T^* \bar{\pi}_T / Z_T$ at final time and, hence, (17) holds for all times $t \in (0, T]$. \square

Lemma 3.1 implies that we can solve the forward evolution equation (18) together with the backward evolution equation (25) instead of the HJB equation (13). Throughout the remainder of this paper, we use

$$(29) \quad \alpha_t(x) = c(x)$$

in line with the previous work [15]. However, other choices could be explored. See, for example, [21], which allows one to incorporate the terminal cost $f(x)$.

Remark 3.1. While [16] and [15] form the basis for our work, we mention the alternative approach put forward in [13], where v_t^* is viewed directly as an unnormalized probability density. This approach leads to the interpretation of the HJB equation (13) in terms of a nonlinear Fokker–Planck equation which in turn can be approximated using interacting particles and EnKF-type approximations as in our work. Only deterministic control problems are considered in [13]. Furthermore, it is not obvious whether the value function v_t^* is always normalizable with respect to the Lebesgue measure on \mathbb{R}^{d_x} .

The final step is to turn (18) and (25), respectively, into forward and reverse McKean–Vlasov SDEs [16]:

$$(30a) \quad d\bar{X}_t = \bar{f}_t^\epsilon(\bar{X}_t)dt + \sqrt{\epsilon}\sigma(\bar{X}_t)dB_t^+, \quad \bar{X}_0 = x,$$

$$(30b) \quad -d\tilde{X}_t = \tilde{f}_t^\epsilon(\tilde{X}_t)dt + \sqrt{\epsilon}\sigma(\tilde{X}_t)dB_t^-, \quad \tilde{X}_T \sim \tilde{\pi}_T.$$

Here B_t^+ denotes Brownian motion adapted to forward time, B_t^- Brownian motion adapted to reverse time, and $\epsilon \in (0, 1]$ is a free parameter determining the noise level added to the McKean–Vlasov equations.

The drift functions are defined as follows:

$$(31) \quad \bar{f}_t^\epsilon(x) := b(x) - \bar{g}_t(x) - \frac{1-\epsilon}{2} (\nabla_x \cdot \Sigma(x) + \Sigma(x) \nabla_x \log \bar{\pi}_t(x))$$

with $\bar{g}_t(x)$ satisfying

$$(32) \quad \nabla_x \cdot (\bar{\pi}_t \bar{g}_t) = -\bar{\pi}_t(c - \bar{\pi}_t[c]),$$

and

$$(33a) \quad \tilde{f}_t^\epsilon(x) := -b(x) + \nabla_x \cdot \Sigma(x) + \Sigma(x) \nabla_x \log \bar{\pi}_t(x) - \tilde{g}_t(x)$$

$$(33b) \quad -\frac{1-\epsilon}{2} (\nabla_x \cdot \Sigma(x) + \Sigma(x) \nabla_x \log \tilde{\pi}_t(x))$$

with $\tilde{g}_t(x)$ satisfying

$$(34) \quad \nabla_x \cdot (\tilde{\pi}_t \tilde{g}_t) = -\tilde{\pi}_t \left(\frac{1}{2} \|\sigma^T \nabla_x \log v_t^*\|^2 - \frac{1}{2} \|RG^T \nabla_x \log v_t^*\|_R^2 - \zeta_t \right).$$

Lemma 3.2. *The two diffusion processes defined by (30) satisfy $\bar{X}_t \sim \bar{\pi}_t$ and $\tilde{X}_t \sim \tilde{\pi}_t$, respectively. Given $\tilde{\pi}_t$ and $\bar{\pi}_t$, the optimal control law $u_t^*(x)$ is provided by*

$$(35) \quad u_t^*(x) = RG(x)^T (\nabla_x \log \tilde{\pi}_t(x) - \nabla_x \log \bar{\pi}_t(x)).$$

Proof. The lemma follows immediately from writing down the associated (nonlinear) Fokker–Planck equations for the two McKean–Vlasov SDEs (30). The stated formula for the optimal control follows from (17). \square

The choice $\epsilon = 0$ leads to fully deterministic evolution equations and the following intriguing representation of (30):

$$(36a) \quad \frac{d\bar{X}_t}{dt} = b(\bar{X}_t) - \bar{g}_t(\bar{X}_t) - \frac{1}{2} (\nabla_x \cdot \Sigma(\bar{X}_t) + \Sigma(\bar{X}_t) \nabla_x \log \bar{\pi}_t(\bar{X}_t))$$

$$(36b) \quad -\frac{d\tilde{X}_t}{dt} = -\tilde{g}_t(\tilde{X}_t) - \bar{g}_t(\tilde{X}_t) - \frac{d\bar{X}_t}{dt}(\tilde{X}_t) + \frac{1}{2} \Sigma(\tilde{X}_t) \nabla_x y_t^*(\tilde{X}_t).$$

We will return to this formulation in Appendix 8.

4. A BRIEF DIVERSION: DIFFUSION-BASED GENERATIVE MODELING

Before discussing numerical implementation of the proposed forward–reverse McKean–Vlasov equations (30), we demonstrate how the core idea of diffusion-based generative

modeling [22, 23], arises as a special instance of (30). Let us start from the control SDE formulation

$$(37) \quad dX_t = -\frac{1}{2}X_t dt + u_t dt + dB_t$$

with initial conditions $X_0 \sim \pi_0 = N(0, I)$. The cost function (2) is implicitly given by

$$(38) \quad e^{-f(x)} \propto \frac{\pi_{\text{data}}(x)}{\pi_0(x)}$$

with running cost $c = 0$ and $R = I$. Here π_{data} denotes the data distribution. We also note that π_0 is the invariant distribution of (37) for $u_t = 0$ and that our forward SDE (30a) simply becomes

$$(39) \quad d\bar{X}_t = -\left(\frac{1}{2}\bar{X}_t - \frac{1-\epsilon}{2}\bar{C}_t^{-1}(\bar{X}_t - \bar{m}_t)\right)dt + \sqrt{\epsilon}dB_t^+, \quad \bar{X}_0 \sim N(0, I).$$

with $\bar{C}_t = I$ and $\bar{m}_t = 0$ for all $t \geq 0$. Furthermore, setting $\epsilon = 0$, leads to

$$(40) \quad \frac{d\bar{X}_t}{dt} = 0.$$

Similarly, the reverse SDE (30b) reduces to

$$(41) \quad -d\tilde{X}_t = -\left(\frac{1}{2}\tilde{X}_t + \frac{1-\epsilon}{2}\nabla_x \log \tilde{\pi}_t(\tilde{X}_t)\right)dt + \sqrt{\epsilon}dB_t^-, \quad \tilde{X}_T \sim \tilde{\pi}_{\text{data}},$$

which is of the standard form used in diffusion modeling for $\epsilon = 1$. The desired control term is finally provided by

$$(42) \quad u_t^*(x) = \nabla_x \log \tilde{\pi}_t(x) + x$$

and the generative SDE model (37) turns into

$$(43) \quad dX_t = \frac{1}{2}X_t dt + \nabla_x \log \tilde{\pi}_t(X_t)dt - \frac{1-\epsilon}{2}\nabla_x \log \pi_t(X_t)dt + \sqrt{\epsilon}dB_t, \quad X_0 \sim N(0, I),$$

which again reduces to the standard diffusion-based generative model for $\epsilon = 1$. A more detailed discussion on the connection between diffusion-based generative modeling and stochastic optimal control can be found in [3].

5. NUMERICAL IMPLEMENTATIONS

In this section, we discuss the numerical implementation of the proposed forward-reverse McKean–Vlasov SDEs (30). We start with Gaussian and EnKF-type approximations [11, 4] before also utilizing diffusion maps [7, 8] in order to approximate the required grad-log density terms.

5.1. EnKF approximation. We develop a numerical implementation of (30) based on the EnKF methodology [11, 4]. In particular, we approximate a drift g_t , which should satisfy

$$(44) \quad \nabla_x \cdot (\pi_t g_t) = -\pi_t(\|\psi\|_B^2 - \pi_t[\|\psi\|_B^2])$$

for given function $\psi(x)$ and density π_t , in the following manner. We introduce the mean, m_t^ψ , of $\psi(x)$ and the covariance matrix, $C_t^{x\psi}$, between x and $\psi(x)$ under π_t . Then an approximative drift term g_t^{KF} is defined by

$$(45) \quad g_t^{\text{KF}}(x) := \frac{1}{2} C_t^{x\psi} B^{-1} \left(\psi(x) + m_t^\psi \right).$$

This approximation becomes exact for Gaussian density π_t and linear function $\psi(x)$. See, for example, [19, 20] for the general methodology and [13] for an application to optimal control.

We assume that the running cost $c(x)$ is of the form (3). Hence, following (32) and (45), the drift term \bar{g}_t is approximated by

$$(46) \quad \bar{g}_t^{\text{KF}}(x) := \frac{1}{2} \bar{C}_t^{xh} S^{-1} \left(h(x) + \bar{m}_t^h \right).$$

Here \bar{C}_t^{xh} denotes the covariance matrix between x and $h(x)$ with respect to $\bar{\pi}_t$ and \bar{m}_t^h the mean of $h(x)$ under the same distribution.

The transformation from \bar{X}_T to \tilde{X}_T under the terminal cost (4) is performed by the stochastic EnKF [11, 4]; that is,

$$(47) \quad \tilde{X}_T = \bar{X}_T - \bar{C}_T^{x\xi} \left(\bar{C}_T^{\xi\xi} + V \right)^{-1} \left(\xi(\bar{X}_T) + V^{1/2} \Xi \right), \quad \Xi \sim \text{N}(0, I).$$

Following the desired control *ansatz* (5), we also approximate $\nabla_x \log v_t^*$ as a linear function using the first two moments of $\tilde{\pi}_t$ and $\bar{\pi}_t$, respectively; that is,

$$(48a) \quad \nabla_x \log v_t^{\text{KF}}(x) := \bar{C}_t^{-1}(x - \bar{m}_t^x) - \tilde{C}_t^{-1}(x - \tilde{m}_t^x)$$

$$(48b) \quad = (\bar{C}_t^{-1} - \tilde{C}_t^{-1})x + \left(\tilde{C}_t^{-1}\tilde{m}_t^x - \bar{C}_t^{-1}\bar{m}_t^x \right) = A_t x + c_t$$

with

$$(49) \quad A_t := \bar{C}_t^{-1} - \tilde{C}_t^{-1}, \quad c_t := \tilde{C}_t^{-1}\tilde{m}_t^x - \bar{C}_t^{-1}\bar{m}_t^x.$$

This approximation leads to the further approximation

$$(50) \quad \tilde{g}_t^{\text{KF}}(x) := \frac{1}{2} \tilde{C}_t A_t \left(\Sigma(\tilde{m}_t^x) - G(\tilde{m}_t^x) R G(\tilde{m}_t^x)^T \right) (A_t x + A_t \tilde{m}_t^x + 2c_t)$$

for the drift term \tilde{g}_t arising from (34).

We now summarize our approximations to the drift terms in the forward-reverse McKean–Vlasov equations (30):

$$(51) \quad \bar{f}_t^\epsilon(x) := b(x) - \frac{1-\epsilon}{2} \left(\nabla_x \cdot \Sigma(x) - \Sigma(x) \bar{C}_t^{-1}(x - \bar{m}_t^x) \right) - \frac{1}{2} \bar{C}_t^{xh} S^{-1} \left(h(x) + \bar{m}_t^h \right)$$

and

$$(52a) \quad \tilde{f}_t^\epsilon(x) := -b(x) + \nabla_x \cdot \Sigma(x) - \Sigma(x) \tilde{C}_t^{-1}(x - \tilde{m}_t^x)$$

$$(52b) \quad - \frac{1-\epsilon}{2} \left(\nabla_x \cdot \Sigma(x) - \Sigma(x) \tilde{C}_t^{-1}(x - \tilde{m}_t^x) \right)$$

$$(52c) \quad - \frac{1}{2} \tilde{C}_t A_t \left(\Sigma(\tilde{m}_t^x) - G(\tilde{m}_t^x) R G(\tilde{m}_t^x)^T \right) (A_t x + A_t \tilde{m}_t^x + 2c_t).$$

The forward equation (30a) is solved from the initial condition $\bar{X}_0 = x_0$. The terminal \bar{X}_T is transformed into the terminal condition \tilde{X}_T using (47). Equation (30b) is solved

from $t = T$ to $t = 0$. The desired approximation to the optimal control u_t^* is provided by (5) with A_t and c_t given by (49). We note that A_t is symmetric negative-definite whenever $\tilde{C}_t \tilde{C}_t^{-1} < I$. In other words, the covariance matrix of the reverse process has to be strictly smaller than the covariance matrix of the forward process in order for the associated control (5) to act in a stabilizing manner.

We also note that the McKean–Vlasov contribution (52c) stabilizes the reverse dynamics provided

$$(53) \quad \Sigma(x) > G(x)RG(x)^T$$

and destabilizes it otherwise. The overall reverse dynamics can still be stable due to the contributions from (52a).

5.2. Combined diffusion map and EnKF approximation. In this subsection, we propose another implementation of the McKean–Vlasov formulation (30) combining the EnKF-type approximations for the drift terms $\bar{g}_t(x)$ and $\tilde{g}_t(x)$, respectively, while using diffusion maps [7, 8] for estimating grad-log density terms.

We first consider the forward McKean–Vlasov equations

$$(54) \quad d\bar{X}_t = b(\bar{X}_t)dt - \frac{1}{2}\bar{C}_t^{xh} \left(h(\bar{X}_t) + \bar{m}_t^h \right) dt + \sigma(\bar{X}_t)dB_t^+.$$

The law $\bar{\pi}_t$ of \bar{X}_t induces the generator $\bar{\mathcal{L}}_t$ at time t , which is defined by

$$(55) \quad \bar{\mathcal{L}}_t f := \frac{1}{\bar{\pi}_t} \nabla_x \cdot (\bar{\pi}_t \Sigma \nabla_x f).$$

Here we assume that $\Sigma(x)$ has full rank. It is easy to verify that

$$(56) \quad \bar{\mathcal{L}}_t \text{Id} = \nabla_x \cdot \Sigma + \Sigma \nabla_x \log \bar{\pi}_t,$$

where $\text{Id} : \mathbb{R}^{d_x} \rightarrow \mathbb{R}^{d_x}$ denotes the identity map; that is, $\text{Id}(x) = x$. Equation (56) suggests the approximation

$$(57) \quad \nabla_x \cdot \Sigma(x) + \Sigma(x) \nabla_x \log \bar{\pi}_t(x) \approx \frac{\exp(\varepsilon \bar{\mathcal{L}}_t) \text{Id} - \text{Id}}{\varepsilon}(x)$$

for $\varepsilon > 0$ sufficiently small, where the semi-group $\exp(\varepsilon \bar{\mathcal{L}}_t)$ will be later replaced by the normalized diffusion map approximation as investigated in [24]. We introduce the conditional mean

$$(58) \quad \bar{m}_t^\varepsilon(x) := \exp(\varepsilon \bar{\mathcal{L}}_t) \text{Id}(x)$$

and obtain the compact representation

$$(59) \quad \frac{\exp(\varepsilon \bar{\mathcal{L}}_t) \text{Id} - \text{Id}}{\varepsilon}(x) = \varepsilon^{-1}(\bar{m}_t^\varepsilon(x) - x).$$

Approximation (57) is plugged into the reverse McKean–Vlasov equation to yield

$$(60a) \quad -d\tilde{X}_t = -b(\tilde{X}_t)dt + \varepsilon^{-1}(\bar{m}_t^\varepsilon(\tilde{X}_t) - \tilde{X}_t)dt - \tilde{g}_t^{\text{KF}}(\tilde{X}_t)dt$$

$$(60b) \quad -\frac{1-\epsilon}{2} \left(\nabla_x \cdot \Sigma(\tilde{X}_t) - \Sigma(\tilde{X}_t) \tilde{C}_t^{-1}(\tilde{X}_t - \tilde{m}_t^x) \right) + \sqrt{\epsilon} \sigma(\tilde{X}_t) dB_t^-,$$

where $\tilde{g}_t^{\text{KF}}(x)$ is defined by (50) as before and $\epsilon \in [0, 1]$.

Approximation (57) can also be used in the forward McKean–Vlasov equation and (54) gets replaced by

$$(61a) \quad d\bar{X}_t = b(\bar{X}_t)dt - \frac{1}{2}\bar{C}_t^{xh} \left(h(\bar{X}_t) + \bar{m}_t^h \right) dt$$

$$(61b) \quad -\frac{1-\epsilon}{2\epsilon}(\bar{m}_t^\epsilon(\bar{X}_t) - \bar{X}_t)dt + \sqrt{\epsilon}\sigma(\bar{X}_t)dB_t^+.$$

Furthermore, the law $\tilde{\pi}_t$ of \tilde{X}_t induces the generator $\tilde{\mathcal{L}}_t$ at time t , which is defined by

$$(62) \quad \tilde{\mathcal{L}}_t f := \frac{1}{\tilde{\pi}_t} \nabla_x \cdot (\tilde{\pi}_t \Sigma \nabla_x f),$$

and which can be used to approximate

$$(63) \quad \nabla_x \cdot \Sigma(x) + \Sigma(x) \nabla_x \log \tilde{\pi}_t(x) \approx \varepsilon^{-1}(\tilde{m}_t^\varepsilon(x) - x), \quad \tilde{m}_t^\varepsilon(x) := \exp(\varepsilon \tilde{\mathcal{L}}_t) \text{Id}(x),$$

in the reverse SDE drift function (33b). In other words, (60) gets replaced by

$$(64a) \quad -d\tilde{X}_t = -b(\tilde{X}_t)dt + \varepsilon^{-1}(\tilde{m}_t^\varepsilon(\tilde{X}_t) - \tilde{X}_t)dt - \tilde{g}_t^{\text{KF}}(\tilde{X}_t)dt$$

$$(64b) \quad -\frac{1-\epsilon}{2\epsilon}(\tilde{m}_t^\varepsilon(\tilde{X}_t) - \tilde{X}_t) + \sqrt{\epsilon}\sigma(\tilde{X}_t)dB_t^-.$$

We note that the McKean–Vlasov equations (61) and (64) become deterministic under the choice $\epsilon = 0$.

5.3. Numerical implementation details. We numerically implement the McKean–Vlasov equations (30) with drift terms given by (51) and (52) using a Monte Carlo approach; that is, we propagate an ensemble of M particles $\bar{X}_t^{(i)}$, $i = 1, \dots, M$, forward in time, $t \in [0, T]$, and an equally sized ensemble of particles $\tilde{X}_t^{(i)}$ backward in time. The required mean values and covariance matrices are replaced by their empirical estimators. A covariance inflation of δI , $\delta > 0$, is added to the empirical covariance matrices in order to ensure that they remain non-singular [11]. For the purpose of this paper, we apply a simple Euler–Maruyama time-stepping method with step-size Δt both in forward and reverse time [14]. More robust time-stepping methods can be based on the formulations proposed and investigated in [1].

When running the EnKF-type formulation from Subsection 5.1, we set the initial conditions to $\bar{X}_0^{(i)} = x_0$ in the forward equation and use $\epsilon > 0$ for the first time-step in order to diffuse these identical particles. All subsequent time-steps employ then $\epsilon = 0$ (deterministic dynamics). The terminal ensemble $\tilde{X}_T^{(i)}$, $i = 1, \dots, M$, is computed using the forward ensemble $\bar{X}_T^{(i)}$ at final time and a standard ensemble implementation of the EnKF update (47) [11, 4]. The reverse McKean–Vlasov equations are solved with $\epsilon = 0$ (deterministic dynamics).

The reverse McKean–Vlasov equation (60) also requires the approximation of the semi-group $\exp(\epsilon \tilde{\mathcal{L}}_t)$. We now describe an implementation which follows ideas from [12]. Based on the forward-in-time samples $\{\bar{X}_t^{(i)}\}$, we first define the diffusion map approximation

$$(65) \quad P_t^\epsilon = D(v_t^\epsilon) R_t^\epsilon D(v_t^\epsilon),$$

where the matrix $R_t^\varepsilon \in \mathbb{R}^{M \times M}$ has entries

$$(66) \quad (R_t^\varepsilon)_{ij} = \exp \left(\frac{-1}{2\varepsilon} (\bar{X}_t^{(i)} - \bar{X}_t^{(j)})^\top \left(\Sigma(\bar{X}_t^{(i)}) + \Sigma(\bar{X}_t^{(j)}) \right)^{-1} (\bar{X}_t^{(i)} - \bar{X}_t^{(j)}) \right),$$

$D(v) \in \mathbb{R}^{M \times M}$ denotes the diagonal matrix with diagonal entries given by the vector $v \in \mathbb{R}^M$, and the vector $v_t^\varepsilon \in \mathbb{R}_+^M$ is chosen such that

$$(67) \quad \sum_{i=1}^M (P_t^\varepsilon)_{ij} = \sum_{j=1}^M (P_t^\varepsilon)_{ij} = \frac{1}{M}.$$

The vector v_t^ε can be computed efficiently using the iterative algorithm from [24].

We define a probability vector $p_t^\varepsilon(x) \in \mathbb{R}^M$ for all $x \in \mathbb{R}^{d_x}$ as follows. First we introduce the vector $r_t^\varepsilon(x) \in \mathbb{R}^M$ with entries

$$(68) \quad (r_t^\varepsilon)_i(x) = \exp \left(\frac{-1}{2\varepsilon} (\bar{X}_t^{(i)} - x)^\top \left(\Sigma(\bar{X}_t^{(i)}) + \Sigma(x) \right)^{-1} (\bar{X}_t^{(i)} - x) \right)$$

for $i = 1, \dots, M$. Next we compute the vector v_t^ε in (65), which in turn is used to define

$$(69) \quad p_t^\varepsilon(x) = \frac{D(v_t^\varepsilon) r_t^\varepsilon(x)}{(v_t^\varepsilon)^\top r_t^\varepsilon(x)}.$$

Setting $\epsilon = \Delta t$, we finally obtain the approximation

$$(70) \quad \bar{m}_t^{\Delta t}(x) = \exp(\Delta t \bar{\mathcal{L}}_t) \text{Id}(x) \approx \bar{\mathcal{X}}_t p_t^{\Delta t}(x)$$

with

$$(71) \quad \bar{\mathcal{X}}_t = \left(\bar{X}_t^{(1)}, \bar{X}_t^{(2)}, \dots, \bar{X}_t^{(M)} \right) \in \mathbb{R}^{d_x \times M}.$$

The reverse McKean–Vlasov equation (60), here with $\epsilon = 1$ for simplicity, is integrated backward in time using the following split-step scheme:

$$(72a) \quad \tilde{X}_{t_{n-1/2}}^{(i)} = \tilde{X}_{t_n}^{(i)} - \Delta t b(\tilde{X}_{t_n}^{(i)}) - \Delta t \tilde{g}_{t_n}^{\text{KF}}(\tilde{X}_{t_n}^{(i)}) dt + \sqrt{\Delta t} \sigma(\tilde{X}_{t_n}^{(i)}) \Xi_{t_n}^{(i)},$$

$$(72b) \quad \tilde{X}_{t_{n-1}}^{(i)} = \bar{\mathcal{X}}_{t_{n-1}} p_{t_{n-1}}^{\Delta t}(\tilde{X}_{t_{n-1/2}}^{(i)}),$$

$i = 1, \dots, M$, where $\Xi_{t_n}^{(i)}$ denote independent standard Gaussian random variables with mean zero and identity covariance matrix, and $t_{n+1} = t_n + \Delta t$. This implementation guarantees that any reverse time solution \tilde{X}_{t_n} is contained in the convex hull generated by the forward samples $\{\bar{X}_{t_n}^{(i)}\}$ [12], which is a desirable property in terms of $\tilde{\pi}_t \propto v_t^* \bar{\pi}_t \ll \bar{\pi}_t$. The approximation (70) can also be applied in the forward McKean–Vlasov equation (61) in case $\epsilon < 1$.

Please note that we propose to still approximate the optimal control $u_t^*(x)$ by (5) with A_t and c_t given by (49). However, diffusion map approximations could also be used in this context. See also [16].

It should be noted that the diffusion map approximation requires $M \gg d_x$, which is in contrast to the EnKF-type approximation from Subsection 5.1, which can be implemented with as little as $M = d_x + 1$ particles in order to render the empirical covariance matrices non-singular and, hence, to obtain well-defined evolution equations at the particle level. This desirable property is verified in the following section. However, EnKF-type approximations can fail due to stability and accuracy reasons and need to then

be augmented by diffusion map approximations as we also demonstrate in the following section.

6. NUMERICAL EXAMPLES

In this section, we discuss numerical findings for two simple control problems. The first control problem is to stabilise the unstable equilibrium position of a mathematical pendulum. This control problem is nonlinear in nature and linear feedback control laws will be suboptimal. However, we find that (5) is nevertheless able to drive the pendulum from the stable to the unstable equilibrium in finite time. The second control problem concerns the stabilization of an unstable equilibrium point of one-dimensional nonlinear Langevin dynamics. Here the computational challenge arises from the fact that the drift term $b(x)$ becomes strongly destabilizing when integrated backward in time which requires a diffusion map approximation of the stabilizing grad-log density term in the reverse McKean–Vlasov dynamics.

6.1. Inverted pendulum. As a first example, we consider the inverted pendulum with control [17]. The state variable is $x = (\theta, \dot{\theta})^T \in \mathbb{R}^2$ with equations of motion

$$(73a) \quad d\theta = \dot{\theta}dt,$$

$$(73b) \quad d\dot{\theta} = \sin(\theta)dt - \cos(\theta)udt + \rho dB_t,$$

and $\rho = 1$. Consider the running cost

$$(74) \quad c(x) = \frac{10}{2} \|\dot{\theta}\|^2$$

over a finite time window $t \in [0, 1]$ with final cost

$$(75) \quad f(x) = \frac{10^3}{2} \|x\|^2.$$

The control is scalar-valued and the penalty term in the cost function uses $R = 10$. Note that $G(x)$ is position dependent and that $(0, 0)$ is an unstable equilibrium point of the deterministic pendulum ($\rho = 0$). The noise acts only on the momentum equation. We seek a control law of the form (5) that leads us from the stable equilibrium $(\pi, 0)$ to the unstable one $(0, 0)$ at time $T = 1$. We initialize $\bar{X}_0 = (\pi, 0.1)$; that is, we give the stable equilibrium a small initial kick.

The numerical experiment uses $M = 3$ ensemble members in the EnKF-type formulation from Subsection 5.1. The time-step is set to $\Delta t = 10^{-4}$ and $\epsilon = 0.01$ for the first time-step of the forward dynamics. The additive covariance inflation factor is set to $\delta = 10^{-4}$. The results from the forward and reverse McKean–Vlasov equations can be found in Figures 1. It can be seen that the forward dynamics stays close to the stable equilibrium point $(\pi, 0)$ over the whole time interval $[0, 1]$. The stiff final cost implied by (75) transforms the ensemble $\bar{X}_T^{(i)}$ to an ensemble $\tilde{X}_T^{(i)}$, $i = 1, \dots, M$, which is tightly clustered about the unstable equilibrium $(0, 0)$ at $T = 1$. Solving the reverse McKean–Vlasov equations leads us gradually back to the unstable equilibrium, which is reached at time $t = 0$.

We then apply the computed control (5) to the inverted pendulum equations (73) with the noise set to zero ($\rho = 0$). The time evolution of the resulting solution is displayed

in Figure 2. The computed time-dependent affine control is able to drive the solution from the stable to the unstable equilibrium point over a unit time interval. The time evolution of the associated velocity indicates that strong acceleration terms are required and indeed provided by the computed control law.

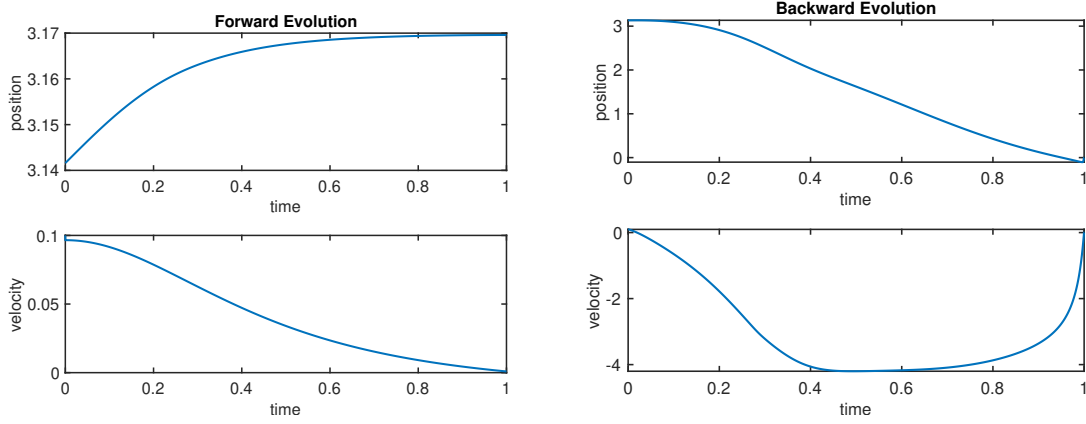


FIGURE 1. Time evolution of the ensemble mean from the forward evolution (left panel) and the reverse evolution (right panel) both in terms of pendulum position and velocity. It can be seen that the reverse evolution connects the stable and unstable equilibrium points while the forward dynamics stays close to the stable equilibrium.

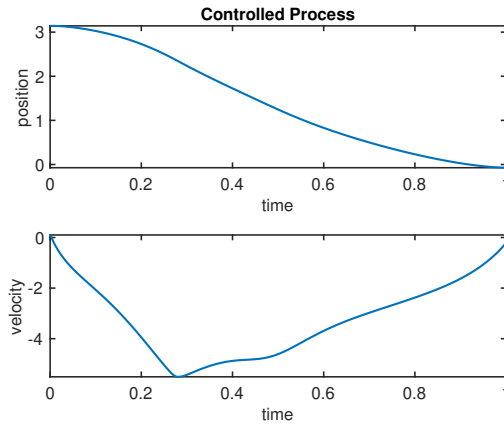


FIGURE 2. Time evolution of the position and velocity of the pendulum under the computed affine control law. The pendulum leaves its initial stable solution to reach the unstable equilibrium at time $T = 1$. The initial and final velocities are essentially zero.

6.2. Controlled Langevin dynamics. As a second example, we consider the controlled Langevin dynamics

$$(76) \quad dX_t = -(X_t^3 - X_t)dt + u_t(X_t)dt + dB_t$$

with unstable equilibrium at $x = 0$ and two stable equilibria at $x = \pm 1$. The imposed running cost is $c(x) = 100x^2/2$ and the terminal cost at $T = 30$ is $f(x) = x^2/2$. We implement the combined diffusion map and EnKF scheme from Subsection 5.2 with step-size $\Delta t = 0.01$, $M = 8$ ensemble members, and $\epsilon = 0$ in the forward (61) and reverse (60) dynamics except for the first ten steps of the forward dynamics (61) where we set $\epsilon = 1$. We also employ additive ensemble inflation with $\delta = 10^{-4}$.

The diffusion map approximation of the grad-log density term in the reverse dynamics is essential for counterbalancing the strongly unstable contribution stemming from the drift term in (76) when integrated backward in time. We also find that the Gaussian approximation to the grad-log density term in the forward dynamics is insufficient and that the diffusion map approximation in (61) significantly improves the behaviour of the deterministic formulation ($\epsilon = 0$). The scale parameter in the diffusion map approximation is set to $\varepsilon = \Delta t$.

Except for brief transition periods at initial and final time, the control law (5) is essentially time-independent. See Figure 3 and the Appendix 8 for a related discussion of infinite horizon optimal control problems. The effectiveness of the control is demonstrated in Figure 4.

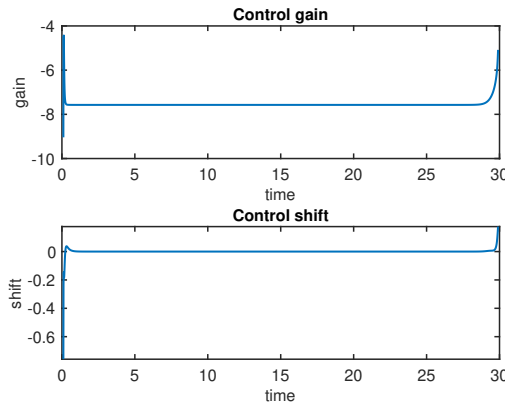


FIGURE 3. Computed control gain A_t and shift c_t from the forward and reverse McKean–Vlasov evolution equations. The control is time-independent except for brief transition periods at the beginning and end of the simulation interval.

7. CONCLUSIONS

Solving the HJB equation numerically constitutes a challenging task. Here we have provided a new perspective by combining forward and reverse evolution McKean–Vlasov equations with the tremendously successful EnKF methodology. We have done so by building on the previous work [15] and have generalized it to a wider class of forward and

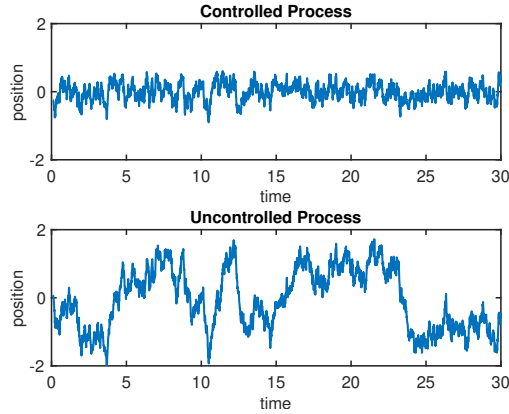


FIGURE 4. Comparison of the controlled and uncontrolled Langevin dynamics. Displayed is the time evolution of a single realisation of the SDE (76) with and without control.

reverse McKean–Vlasov equations. In order to keep those equations computationally tractable we have employed EnKF-type approximations to the McKean–Vlasov interaction terms. While not delivering optimal control laws, the resulting time-dependent affine control laws can either be sufficient in themselves or, alternatively, may provide the starting point for more accurate approximations such as the diffusion map approach outlined in Subsection 5.2. We have applied the proposed methodology to a two-dimensional nonlinear control problem using only $M = d_x + 1 = 3$ particles. Such a small ensemble size constitutes a significant improvements over the results presented in [15] and [13]. It remains to be demonstrated that the methodology can be further extended to high-dimensional control problems in the spirit of EnKF applications to data assimilation, which deliver useful approximations even with $M \ll d_x$ ensemble members [11]. At the same time, strongly nonlinear Langevin dynamics (76) requires more sophisticated approximations of the grad-log terms in terms of diffusion maps. Still the ensemble size could be kept at a moderate level ($M = 8$) in order to recover the linear control law (5) robustly.

Acknowledgment. This work has been funded by Deutsche Forschungsgemeinschaft (DFG) - Project-ID 318763901 - SFB1294. The author thanks Manfred Opper for insightful discussions on the subject of this work.

8. APPENDIX

In this appendix, we discuss an extension of the proposed methodology to infinite horizon control problems with cost function

$$(77) \quad J_\infty(x_0, u_{0:\infty}) = \mathbb{E} \left[\int_0^\infty e^{-\gamma t} \left(c(X_t) + \frac{1}{2} \|u_t\|_R^2 \right) dt \right].$$

Here $\gamma \geq 0$ denotes the discount factor. The associated transformed HJB equation becomes

$$(78a) \quad -\partial_t v_t^* = b \cdot \nabla_x v_t^* + \frac{1}{2} \Sigma : D_x^2 v_t^*$$

$$(78b) \quad - \left(c + \gamma \log v_t^* + \frac{1}{2} \|\sigma^T \nabla_x \log v_t^*\|^2 - \frac{1}{2} \|RG^T \nabla_x \log v_t^*\|_R^2 \right) v_t^*$$

with terminal condition $v_\infty^* = 1$.

The only modification to the finite horizon formulations from Section 3 concerns the drift function (33), where $\tilde{g}_t(x)$ has to now satisfy the Poisson equation

$$(79) \quad \nabla_x \cdot (\tilde{\pi}_t \tilde{g}_t) = -\tilde{\pi}_t \left(\gamma \log v_t^* + \frac{1}{2} \|\sigma^T \nabla_x \log v_t^*\|^2 - \frac{1}{2} \|RG^T \nabla_x \log v_t^*\|_R^2 - \zeta_t \right)$$

and the EnKF-based approximation of \tilde{g}_t becomes

$$(80) \quad \tilde{g}_t^{\text{KF}}(x) := \frac{1}{2} \tilde{C}_t \left\{ \gamma I + A_t (\Sigma(\tilde{m}_t^x) - G(\tilde{m}_t^x) R G(\tilde{m}_t^x)^T) \right\} (A_t x + A_t \tilde{m}_t^x + 2c_t).$$

Please note that $\tilde{C}_t A_t = \tilde{C}_t \bar{C}_t^{-1} - I < 0$ under the assumption that $\tilde{C}_t < \bar{C}_t$. Hence, the additional drift term stabilizes the time evolution of the reverse covariance matrix \tilde{C}_t towards \bar{C}_t .

One expects the forward process (36a) to reach an equilibrium distribution with mean \bar{m}_{eq} and covariance matrix \bar{C}_{eq} for $t > 0$ sufficiently large. Furthermore, upon setting $\epsilon = 0$ in (30) and since we are in equilibrium, the time derivative $d\bar{X}_t/dt$ will either be zero or can be assumed to be relatively small. One may then fix these quantities in the reverse process (36b)-(36c), which, in turn, is integrated backward in time till an equilibrium distribution is reached with mean \tilde{m}_{eq} and covariance matrix \tilde{C}_{eq} . The optimal control is provided by

$$(81) \quad u_t^*(x) = RG(x)^T \left(\bar{C}_{\text{eq}}^{-1}(x - \bar{m}_{\text{eq}}^x) - \tilde{C}_{\text{eq}}^{-1}(x - \tilde{m}_{\text{eq}}^x) \right).$$

Such a methodology provides an approximation to the stationary solution of the HJB equation (78).

The combined EnKF and diffusion map approximation formulation from Section 5.2 can be generalized to the infinite horizon optimal control problem in a similar fashion. Please note that the numerical results from Subsection 6.2 already implied an essentially time-independent control law.

Alternatively, one can follow the actor-critic methodology to stochastic optimal control [17] and introduce a family of control laws $u_\theta(x)$ parametrized by $\theta \in \mathbb{R}^{d_\theta}$ and set $\gamma = 0$ in (77). For example, using a (stationary) linear control law of the form (5), the adjustable parameters, θ , would be given by the (constant) matrix A_t and the (constant) vector c_t .

More specifically, the actor chooses parameters, θ , and considers the controlled SDE

$$(82) \quad dX_t = b(X_t)dt + G(X_t)u_\theta(X_t)dt + \sigma(X_t)dB_t.$$

The generator of this SDE is denoted by \mathcal{L}_θ . It is assumed that the SDE possesses an invariant density π_θ ; that is,

$$(83) \quad \mathcal{L}_\theta^\dagger \pi_\theta = 0,$$

where $\mathcal{L}_\theta^\dagger$ denotes the adjoint of \mathcal{L}_θ [18]. The optimal θ_* is determined by

$$(84) \quad \theta_* = \arg \min_{\theta} \pi_\theta[c_\theta]$$

with cost

$$(85) \quad c_\theta(x) = c(x) + \frac{1}{2} \|u_\theta(x)\|_R^2.$$

The critic provides the value function y_θ , which satisfies the stationary HJB equation

$$(86) \quad \mathcal{L}_\theta y_\theta + c_\theta - \pi_\theta[c_\theta] = 0.$$

Given the value function $y_\theta(x)$, the chosen parameter, θ , can now be improved using the gradient [17]

$$(87) \quad \nabla_\theta \pi_\theta[c_\theta] = \pi_\theta [(\nabla_\theta \mathcal{L}_\theta) y_\theta] + \pi_\theta [\nabla_\theta c_\theta] = \pi_\theta [\nabla_\theta u_\theta^\top (G^\top \nabla_x y_\theta + u_\theta)]$$

and the optimal parameter value satisfies $\nabla_\theta \pi_{\theta_*}[c_{\theta_*}] = 0$.

In order to extend our McKean–Vlasov approach to this control setting, we replace the stationary HJB equation (86) by the forward-in-time HJB equation

$$(88) \quad \partial_t y_t = \mathcal{L}_\theta y_t + c_\theta - \pi_\theta[c_\theta]$$

and apply the transformation $v_t(x) = \exp(-y_t(x))$ to obtain the modified HJB equation

$$(89) \quad \partial_t v_t = \mathcal{L}_\theta v_t - \left(c_\theta + \frac{1}{2} \|\sigma^\top \nabla_x \log v_t\|^2 - \zeta_t \right) v_t$$

for $t \geq 0$ with initial condition $v_0(x) = 1$ and ζ_t an appropriate normalization constant.

Adapting our previously developed methodology, we introduce the density

$$(90) \quad \tilde{\pi}_t(x) := Z_t^{-1} v_t(x) \pi_\theta(x)$$

with $Z_t = \pi_\theta[v_t]$ and find that

$$(91) \quad \nabla_x y_\theta = \nabla_x \log \pi_\theta - \lim_{t \rightarrow \infty} \nabla_x \log \tilde{\pi}_t.$$

Furthermore, the density $\tilde{\pi}_t$ satisfies the forward evolution equation

$$(92a) \quad \partial_t \tilde{\pi}_t = -\nabla_x \cdot (\tilde{\pi}_t \tilde{b}_\theta) + \frac{1}{2} \nabla_x \cdot (\nabla_x \cdot (\tilde{\pi}_t \Sigma)) - \tilde{\pi}_t \left(c_\theta + \frac{1}{2} \|\sigma^\top \nabla_x \log v_t\|^2 - \tilde{\zeta}_t \right)$$

$$(92b) \quad = -\mathcal{L}_\theta \tilde{\pi}_t + \nabla_x \cdot (\tilde{\pi}_t \nabla_x \log v_t) - \tilde{\pi}_t \left(c_\theta + \frac{1}{2} \|\sigma^\top \nabla_x \log v_t\|^2 - \tilde{\zeta}_t \right),$$

with modified drift function

$$(93) \quad \tilde{b}_\theta(x) := -b(x) - G(x)u_\theta(x) + \nabla_x \cdot \Sigma(x) + \Sigma(x) \nabla_x \log \pi_\theta(x)$$

and normalisation constant $\tilde{\zeta}_t$. The associated forward McKean–Vlasov evolution equation is for $\epsilon = 0$ given by

$$(94) \quad \frac{d\tilde{X}_t}{dt} = \tilde{b}_\theta(\tilde{X}_t) - \tilde{g}_t(\tilde{X}_t) - \frac{1}{2} (\nabla_x \cdot \Sigma(x) + \Sigma(x) \nabla_x \log \tilde{\pi}_t(x)),$$

with initial $\tilde{X}_0 \sim \pi_\theta$ and the McKean–Vlasov drift term $\tilde{g}_t(x)$ has to now satisfy

$$(95) \quad \nabla_x \cdot (\tilde{\pi}_t \tilde{g}_t) = -\tilde{\pi}_t \left(c_\theta + \frac{1}{2} \|\sigma^\top \nabla_x \log v_t\|^2 - \tilde{\zeta}_t \right).$$

We may assume that (92) possesses an invariant density $\tilde{\pi}_\theta$. Then (91) reduces to

$$(96) \quad \nabla_x y_\theta = \nabla_x \log \pi_\theta - \nabla_x \log \tilde{\pi}_\theta.$$

Using (91), the chosen parameters can be improved via standard gradient descent based upon the gradient (87) giving rise to time-dependent parameters, θ_t , which, under suitable assumptions, converge to the optimal θ_* . Furthermore, provided the parameters are adjusted slowly enough in time, one can make the assumption that $\mathcal{L}_{\theta_t} \pi_{\theta_t} \approx 0$. These assumptions suggest the coupled set of forward McKean–Vlasov evolution equations

$$(97a) \quad \frac{dX_t}{dt} = b(X_t) + G(X_t)u_{\theta_t}(X_t) - \frac{1}{2}\nabla_x \cdot \Sigma(X_t) - \frac{1}{2}\Sigma(X_t)\nabla_x \log \pi_t(X_t),$$

$$(97b) \quad \frac{d\tilde{X}_t}{dt} = -b(\tilde{X}_t) - G(\tilde{X}_t)u_\theta(\tilde{X}_t) + \frac{1}{2}\nabla_x \cdot \Sigma(\tilde{X}_t) + \Sigma(\tilde{X}_t)\nabla_x \log \pi_t(\tilde{X}_t) - \tilde{g}_t(\tilde{X}_t)$$

$$(97c) \quad -\frac{1}{2}\Sigma(\tilde{X}_t)\nabla_x \log \tilde{\pi}_t(\tilde{X}_t),$$

$$(97d) \quad \frac{d\theta_t}{dt} = -\delta (\pi_t [(\nabla_\theta \mathcal{L}_{\theta_t})y_t] + \pi_t [\nabla_\theta c_{\theta_t}]) = -\delta \pi_t [\nabla_\theta u_{\theta_t}^\top (G^\top \nabla_x y_t + u_{\theta_t})]$$

where $\delta > 0$ is sufficiently small, $\tilde{g}_t(x)$ satisfies (95), and

$$(98) \quad \nabla_x y_t(x) := \nabla_x \log \pi_t(x) - \nabla_x \log \tilde{\pi}_t(x).$$

Here π_t denotes the law of X_t and $\tilde{\pi}_t$ the law of \tilde{X}_t . The numerical approximations introduced in Section 5 can now be applied to this system of McKean–Vlasov SDEs as well.

In line with the previously stated (36), we note that (97b) can be rewritten in the form

$$(99) \quad \frac{d\tilde{X}_t}{dt} = -\tilde{g}_t(\tilde{X}_t) - \frac{dX_t}{dt}(\tilde{X}_t) + \frac{1}{2}\Sigma(\tilde{X}_t)\nabla_x y_t(\tilde{X}_t).$$

In this context, it is worthwhile to consider the special case $G = R = I$, $\Sigma = 2I$, $b(x) = -\nabla_x U(x)$, and $u_\theta(x) = -\nabla_x \Psi_\theta(x)$ in more detail. Here $U(x) : \mathbb{R}^{d_x} \rightarrow \mathbb{R}$ and $\Psi_\theta(x) : \mathbb{R}^{d_x} \rightarrow \mathbb{R}$ are given functions. Under these assumptions, the density π_θ is explicitly known and

$$(100) \quad \nabla_x \log \pi_\theta(x) = -\nabla_x U(x) - \nabla_x \Psi_\theta(x).$$

Furthermore, we may assume that (97a) is in equilibrium and we can set

$$(101) \quad \frac{dX_t}{dt} \equiv 0$$

in (99). Let $\tilde{g}_t(x) = \nabla_x V_t(x)$ denote the solution of (95) for appropriate potential $V_t(x)$, then it follows from (99) and $d\tilde{X}_t/dt \approx 0$ that

$$(102) \quad \nabla_x y_t(x) \approx \nabla_x V_t(x).$$

Hence,

$$(103) \quad \pi_t [(\nabla_\theta \mathcal{L}_{\theta_t})y_t] + \pi_t [\nabla_\theta c_{\theta_t}] \approx \pi_{\theta_t} [\nabla_\theta (\nabla_x \Psi_{\theta_t})^\top (\nabla_x V_t + \nabla_x \Psi_{\theta_t})]$$

and the optimal parameter choice, θ_* , satisfies

$$(104) \quad 0 = \pi_{\theta_*} [\nabla_\theta (\nabla_x \Psi_{\theta_*})^\top (\nabla_x V_{\theta_*} + \nabla_x \Psi_{\theta_*})]$$

subject to the potential $V_{\theta_*}(x)$ satisfying the Poisson equation

$$(105) \quad \nabla_x \cdot (\tilde{\pi}_{\theta_*} \nabla_x V_{\theta_*}) = -\tilde{\pi}_{\theta_*} (c_{\theta_*} + \|\nabla_x V_{\theta_*}\|^2 - \zeta_*)$$

with $\tilde{\pi}_{\theta_*} \propto e^{-V_{\theta_*}} \pi_{\theta_*}$. The approach proposed in this paper can now be viewed as providing a dynamic particle-based algorithm for solving the nonlinear equations (104)-(105). It is also worth noting that (105) is equivalent to

$$(106) \quad \mathcal{L}_{\theta_*} V_{\theta_*} = -c_{\theta_*} + \pi_{\theta_*}[c_{\theta_*}],$$

which implies $\nabla_x y_{\theta_*} = \nabla_x V_{\theta_*}$ as desired.

REFERENCES

- [1] Javier Amezcua, Eugenia Kalnay, Kayo Ide, and Sebastian Reich. Ensemble transform Kalman-Bucy filters. *Q.J.R. Meteor. Soc.*, 140:995–1004, 2014.
- [2] Brian D.O. Anderson. Reverse-time diffusion equation models. *Stochastic Processes Applications*, 12:313–326, 1982.
- [3] Julius Berner, Lorenz Richter, and Karen Ullrich. An optimal control perspective on diffusion-based generative modeling. *preprint arXiv:2211.01364*, 2023.
- [4] Edoardo Calvello, Sebastian Reich, and Andrew M. Stuart. Ensemble Kalman methods: A mean field perspective. *preprint arXiv:2209.11371*, 2022.
- [5] René Carmona. *Lectures on BSDEs, Stochastic Control, and Stochastic Differential Games with Financial Applications*. SIAM, Philadelphia, 2016.
- [6] Jared Chessari, Reiichiro Kawai, Yuji Shinozaki, and Toshihiro Yamada. Numerical methods for backward stochastic differential equations: A survey. *preprint arXiv:2101.08936*, 2021.
- [7] R. R. Coifman, S. Lafon, A. B. Lee, M. Maggioni, B. Nadler, F. Warner, and S. W. Zucker. Geometric diffusions as a tool for harmonic analysis and structure definition of data: Diffusion maps. *Proceedings of the National Academy of Sciences*, 102(21):7426–7431, 2005.
- [8] Ronald R. Coifman and Stéphane Lafon. Diffusion maps. *Applied and Computational Harmonic Analysis*, 21(1):5–30, 2006. Special Issue: Diffusion Maps and Wavelets.
- [9] Weinan E, Jiequn Han, and Arnulf Jentzen. Deep learning-based numerical methods for high-dimensional parabolic partial differential equations and backward stochastic differential equations. *Communications in Mathematics and Statistics*, 5:349–380, 2017.
- [10] Weinan E, Jiequn Han, and Arnulf Jentzen. Algorithms for solving high-dimensional PDEs: From nonlinear Monte Carlo to machine learning. *Nonlinearity*, 35:278, 2021.
- [11] Geir Evensen, Femke C. Vossepoel, and Peter Jan. van Leeuwen. *Data Assimilation Fundamentals: A unified Formulation of the State and Parameter Estimation Problem*. Springer Nature Switzerland AG, Cham, Switzerland, 2022.
- [12] Georg Gottwald, Fengyi Li, Youssef Marzouk, and Sebastian Reich. Stable generative modeling using diffusion maps. *preprint arXiv:2401.04372*, 2024.
- [13] Anant A. Joshi, Amirhossein Taghvaei, Prashant G. Mehta, and Sean P. Meyn. Controlled interacting particle algorithms for simulation-based reinforcement learning. *Systems & Control Letters*, 170:105392, 2022.

- [14] Peter Kloeden and Eckhard Platen. *Numerical methods for stochastic differential equations*. Springer, New York, 1991.
- [15] Dimitra Maoutsa and Manfred Opper. Deterministic particle flows for constraining stochastic nonlinear systems. *Phys. Rev. Res.*, 4:043035, 2022.
- [16] Dimitra Maoutsa, Sebastian Reich, and Manfred Opper. Interacting particle solutions of Fokker–Planck equations through gradient-log-density estimation. *Entropy*, 22(8), 2020.
- [17] Sean Meyn. *Control Systems and Reinforcement Learning*. Cambridge University Press, Cambridge, 2022.
- [18] Grigorios A. Pavliotis. *Stochastic Processes and Applications*. Springer Verlag, New York, 2016.
- [19] Sebastian Reich. A dynamical systems framework for intermittent data assimilation. *BIT Numerical Mathematics*, 51(1):235–249, 2011.
- [20] Sebastian Reich. Data assimilation: The Schrödinger perspective. *Acta Numerica*, 28:635–711, 2019.
- [21] Sebastian Reich. Data assimilation: A dynamic homotopy-based coupling approach. In Bertrand Chapron, Dan Crisan, Darryl Holm, Etienne Mémin, and Anna Radomska, editors, *Stochastic Transport in Upper Ocean Dynamics II*, pages 261–280, Cham, 2024. Springer Nature Switzerland.
- [22] Jascha Sohl-Dickstein, Eric Weiss, Niru Maheswaranathan, and Surya Ganguli. Deep unsupervised learning using nonequilibrium thermodynamics. In *International Conference on Machine Learning*, pages 2256–2265. PMLR, 2015.
- [23] Yang Song, Jascha Sohl-Dickstein, Diederik P Kingma, Abhishek Kumar, Stefano Ermon, and Ben Poole. Score-based generative modeling through stochastic differential equations. In *International Conference on Learning Representations*, 2021. URL: <https://openreview.net/forum?id=PXTIG12RRHS>.
- [24] C.L. Wormell and S. Reich. Spectral convergence of diffusion maps: Improved error bounds and an alternative normalisation. *SIAM J. Numer. Anal.*, 59:1687–1734, 2021.